Making a pathogen? Evaluating the impact of protist predation on the evolution of virulence in *Serratia marcescens*

Heather A. Hopkins[1,2], Christian Lopezguerra[1,2], Meng-Jia Lau[1], Kasie Raymann[1,2*]

1. Department of Plant and Microbial Biology, North Carolina State University
2. Department of Biology, University of North Carolina Greensboro

*Kasie Raymann

Email: ktrayman@ncsu.edu

Keywords: evolution, exaptation, virulence, predation, bacteria, opportunistic pathogen

Abstract

Opportunistic pathogens are environmental microbes that are generally harmless and only occasionally cause disease. Unlike obligate pathogens, the growth and survival of opportunistic pathogens does not rely on host infection or transmission. Their versatile lifestyles make it challenging to decipher how and why virulence has evolved in opportunistic pathogens. The Coincidental Evolution Hypothesis (CEH) postulates that virulence results from exaptation or pleiotropy, i.e., traits evolved for adaptation to living in one environment that have a different function in another. In particular, adaptation to avoid or survive protist predation has been suggested to contribute to the evolution of bacterial virulence (the training grounds hypothesis). Here we used experimental evolution to determine how the selective pressure imposed by a protist predator impacts the virulence and fitness of a ubiquitous environmental opportunistic bacterial pathogen that has acquired multi-drug resistance: *Serratia marcescens*. To this aim, we evolved *S. marcescens* in the presence or absence of generalist protist predator, *Tetrahymena thermophila*. After 60 days of evolution, we evaluated genotypic and phenotypic changes by comparing evolved *S. marcescens* to the ancestral strain. Whole genome shotgun (WGS) sequencing of the entire evolved populations and individual isolates revealed numerous cases of parallel evolution, many more than statistically expected by chance, in genes associated with virulence. Our phenotypic assays suggested that evolution in the presence of a predator maintained virulence, whereas evolution in the absence of a predator resulted in attenuated virulence. We also found a significant correlation between virulence, biofilm formation, and grazing resistance. Overall, our results provide evidence that bacterial virulence and virulence related traits are maintained by selective pressures imposed by protist predation.

Introduction

Opportunistic pathogens are environmental bacteria that typically coexist peacefully alongside hosts and only sometimes cause disease, e.g., in hosts with immunodeficiency or microbiome imbalance (1). Opportunistic pathogens are intriguing because they have diverse lifestyles and experience strong tradeoffs between adaptation to life in the environment versus life inside of a host (1–3). Opportunistic pathogens are also conceptually challenging because, unlike obligate pathogens, their survival does not depend on their ability to infect a host: they are fully capable of reproducing and living in the environment (1, 4). Thus, the factors driving virulence in opportunistic pathogens remain largely enigmatic from an evolutionary standpoint. Several hypotheses have been put forth, proposing that virulence is selected for, or maintained by, interactions that occur outside a host. The Coincidental Evolution Hypothesis (CEH) postulates that virulence evolves indirectly due to selection that occurs in non-host environments (5, 6), and protists have been proposed to act as “Trojan Horses” (7) or training grounds (8) for the evolution of bacterial pathogens. These hypotheses stem from the fact that bacterial defense mechanisms against environmental predators (e.g., protists) such as adherence, biofilm formation, grazing resistance, intracellular toxin production, and outer-membrane structures also play a role in host infection (1, 9, 10). Additionally, several studies have shown that pathogens challenged with microbial predators exhibited increased host virulence (11–16).

Experimental evolution can help reveal how different environmental pressures impact the evolution of bacteria and which genes are involved in specific phenotypic traits (17–19). In recent years, experimental evolution has been used to investigate if eukaryotic predation increases the virulence of opportunistic bacterial pathogens, but results have been conflicting (20–26). One major limitation of many previous studies has been the lack of thorough phenotypic and genotypic characterization. Not all populations will follow the same evolutionary trajectory (27–31). Therefore, evaluating and comparing genotype and multiple phenotypes in experimental evolution studies is critical. For example, even if predation generally selects for the maintenance or enhancement of pathogen virulence, it is possible that some traits that are adaptive for defense against predators have no impact on virulence or even result in attenuation of pathogenicity within hosts. Nevertheless, experimental evolution can be used to answer many questions about fundamental evolutionary processes (17–19) and help reveal genes and mechanisms associated with virulence and other phenotypes. Thus, the goal of this study was to experimentally evolve the opportunistic bacterial pathogen *Serratia marcescens* in the presence or absence of an environmental protist predator and characterize both the genotypes and phenotypes of

67 the evolved bacteria to elucidate how predation, or the lack thereof, impacts opportunistic pathogen
68 evolution. We hypothesized that virulence would be increased or at least maintained in the presence of
69 a predator.

70 *S. marcescens* is an opportunistic pathogen that ubiquitously occurs in soil and water (32) and
71 has been used for several bacteria-predator experimental evolution studies (20, 21, 23). It is a host
72 generalist that can colonize many different organisms, where it can be pathogenic and/or commensal
73 (32). In humans, *S. marcescens* is a common enteric bacterium that is generally harmless in the
74 gastrointestinal tract (33). However, it was recently found to be capable of damaging gut epithelial cells
75 *in vitro* (34) and is responsible for causing dangerous nosocomial infections worldwide, notably in the
76 respiratory and urinary tracts (35, 36). In the last few decades, the frequency of nosocomial infections
77 caused by *S. marcescens* has increased, several hospital-wide outbreaks have been reported, and
78 most strains have acquired multidrug resistance (35–37). Additionally, *S. marcescens* has been
79 recognized as an opportunistic pathogen of many plants and other animals (32). Thus, understanding
80 the evolution of virulence in *S. marcescens* is important for the health of a wide range of organisms. In
81 this study, we used *S. marcescens* KZ19 (38), which was isolated from the gut of a honey bee (*Apis*
82 *mellifera*) and is pathogenic to honey bees following microbiome disruption (39–42) or if administered
83 orally to bees at high doses (38). This strain of *S. marcescens* resides in a monophyletic clade with
84 human and plant isolates, with the closest sequenced relative being a nosocomial strain BIDMC 50
85 (38).

86 Here, we serially passaged *S. marcescens* KZ19 every day for 60 days in the presence or
87 absence of a generalist protist predator, *Tetrahymena thermophila* (Figure 1). Following 60 days of
88 evolution, we performed whole genome shotgun (WGS) metagenomic sequencing on the entire *S.*
89 *marcescens* evolved populations, sequenced individual evolved isolates, and characterized the
90 mutations present in both evolved isolates and populations. We observed multiple cases of parallel
91 evolution which, when combined with phenotypic assays of isolates, enabled us to predict genes and
92 pathways involved in virulence-related phenotypes. Although all populations did not follow the same
93 evolutionary trajectories, in general, we found that virulence and grazing resistance was attenuated in
94 the absence of a predator and predation resulted in increased biofilm production and slightly elevated
95 virulence. Additionally, we found strong correlations between predation (grazing) resistance, biofilm
96 production, and pathogenicity (in honey bees), lending support to the hypothesis that predation
97 resistance and virulence are often governed by the same mechanisms. In conclusion, our study

98 provides evidence that experimental evolution can be used to help elucidate how exposure to non-host
99 environments impacts opportunistic pathogen evolution.

100 **Results**

101 We confirmed that *T. thermophila* grazes on the ancestral bacterial strain by visualizing a 24h
102 co-culture of *T. thermophila* and a transconjugant *S. marcescens* KZ19 containing an E2 crimson
103 fluorescent protein (38, 43) via fluorescent microscopy (Figure 1). We then created six media-evolved
104 (ME) and six predator-evolved (PE) replicate Lines (populations). We minimized predator/prey co-
105 evolution by passaging evolved *S. marcescens* to new axenic *T. thermophila* cultures each day. The
106 same concentration of *S. marcescens* was transferred for each passage, and we confirmed successful
107 passaging via plating on LB agar every day. Viability and population size of *T. thermophila* was
108 evaluated before every passage via light microscopy. Following 60 days of evolution the entire PE
109 (*n*=6) and ME populations (*n*=6) were sequenced using WGS metagenomic sequencing. The ancestor
110 (*n*=1) and individual isolates from the three ME (Lines 1-3) and six PE (Lines 1-6) populations were
111 sequenced using WGS sequencing (Table S1). We then performed phenotypic assays on the evolved
112 isolates (ME=3 and PE=6) in order to associate mutations with phenotypes.

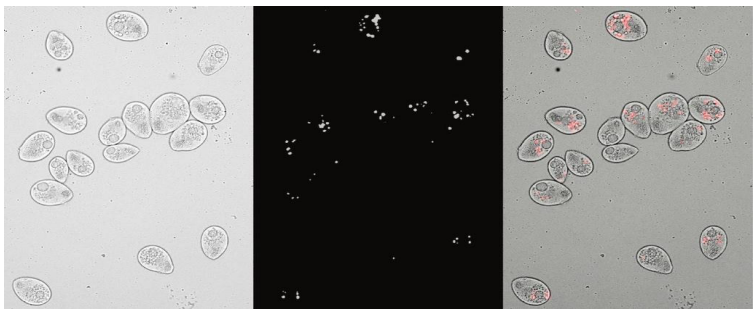

113

114 **Figure 1**. Confirmation of grazing activity. A) Phase contrast image of *T. thermophila* after 24h co-culture with fluorescently
115 labeled *S. marcescens* KZ19 in Neff media with 180 ug/ml spectinomycin, B) Cy5 filter image showing the E2 crimson labeled
116 *S. marcescens* KZ19 cells inside *T. thermophila*, and C) composite overlay of the phase contrast and fluorescent images.
117 Images were taken at 20X on a Keyence BZ-X700 Series All-In-One Fluorescence Microscope and overlayed in ImageJ.

118 *Mutations in the predator- and media-evolved populations*

119 All evolved populations were compared to the ancestral genome to identify mutations. First, the
120 ancestral genome was re-sequenced using both long (Nanopore) and short (Illumina) read sequencing
121 technologies and assembled using SPades v3.15.3 (44) to generate a consensus ancestral genome
122 (Table S1). We then corrected for false positives (i.e., sequencing errors) by mapping all the short
123 reads (244X coverage) of the ancestral strain back to the new consensus ancestral genome using
124 BreSeq v0.38.2 (45). All mutations predicted via BreSeq (45) when the ancestral reads were mapped to

125 the ancestral consensus genome were considered false positives if detected in the evolved populations
126 (i.e., they most likely correspond to sequencing or assembly issues in the ancestral genome).

127 We first analyzed the mutation patterns across each population. The total number of mutations
128 identified in each evolved population (ME_p n=6; PE_p n=6) ranged from 6 to 106 (minimum frequency
129 cutoff of 0.05) with an average of 44 mutations per population (Supplemental Dataset 1). The
130 population with the lowest mutations identified was ME_p3 and the two with the largest number of
131 mutations were PE_p3 and ME_p2. However, the number of mutations present in a population was
132 negatively correlated to the average genome coverage (P= 0.0001, R^2=0.7805; Figure S1). A negative
133 correlation between the number of mutations and genome coverage indicates that our sequencing
134 depth was sufficient to characterize the mutations present in the populations.

135 In all evolved populations we identified nonsynonymous, synonymous, and intergenic mutations
136 (Figure 2A, Supplemental Dataset 1). To determine the percentage of nonsynonymous, synonymous,
137 intergenic, non-sense, and RNA mutations expected at random, we simulated independent mutations in
138 the ancestral *S. marcescens* KZ19 genome by performing 10,000 independent simulations using a
139 Jukes & Cantor model (47). We found that the percentage of nonsynonymous mutations detected in our
140 populations (49-68%) was between 4-23% less than the random expectation of 71.5% (Figure 2A),
141 indicating that overall, both environments imposed negative (purifying) selective pressure on *S.*
142 *marcescens* (i.e., deleterious mutations are being purged).

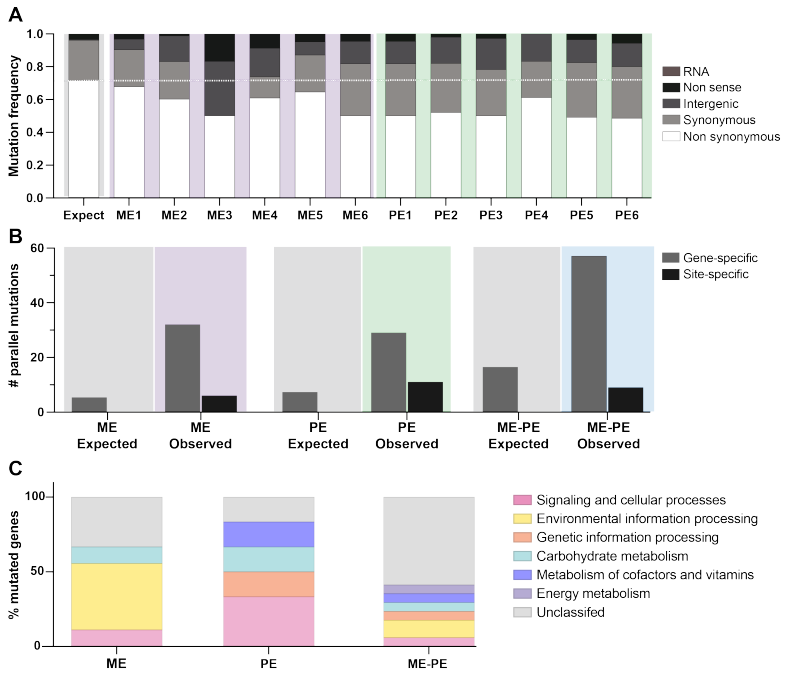

Figure 2. Characterization of the mutations present in the evolved populations **A)** Percentage of nonsynonymous, synonymous, intergenic, non-sense, and RNA mutations detected in each evolved population (ME1-6 and PE1-6) and compared to the percentage of each mutation type expected at random (Expected). **B)** Number of observed parallel (*gene-* and *site-specific*) mutation events observed in ME, PE, and in both ME and PE (ME-PE) populations compared to random expectation (expected vs. observed). Significantly more *gene-specific* and *site-specific* parallel mutations were observed than would be expected to occur by chance (Chi-squared test, P<0.0001). **C)** the KEGG (46) functional annotations of the genes in which parallel events occurred.

144

145 In addition to purifying selection, we also found evidence that our populations were undergoing
146 positive selection based on the identification of numerous mutations either in the exact same position
147 (*site-specific* parallel evolution) or in the same gene (*gene-specific* parallel evolution) across
148 populations (Figure 2B, Supplemental Dataset 1). Parallel evolution events were considered if a
149 mutation was found in the same position or gene in independently evolved populations (ME_p, PE_p, or
150 both). None of the parallel evolution events occurred across all populations, confirming that they were
151 not present in the ancestral population. We observed a total of 118 parallel mutations; 57 (nine *same-*
152 *site*) were shared between the ME_p and PE_p populations, 29 (11 *same-site*) were unique to PE_p
153 populations, and 32 (six *same-site*) were unique to ME_p populations (Figure 2B, Supplemental Dataset
154 1).

155 To determine the number of parallel mutations expected to occur by chance we simulated
156 independent mutations in the ancestral *S. marcescens* KZ19 genome by performing 10,000
157 independent simulations using a Jukes & Cantor model (47). The number of *site-specific* parallel
158 mutations expected to occur by chance within or across all our evolved populations was less than one,
159 indicating that we found overwhelmingly more site-specific parallel mutations than random expectation
160 (Figure 2B, ME_p P=2.2e-16, PE_p P= 2.2e-16 , ME_p-PE_p P= 2.2e-16, Chi-squared test). The number of
161 *gene-specific* parallel mutations observed across the ME_p and PE_p populations was also four times
162 more frequent than expected at random (Figure 2B, ME_p P= 8.7e-25, PE_p P= 6.2e-05, ME_p-PE_p P=
163 6.4e-10, Chi-squared test). The presence of excessive convergent parallel mutations provides strong
164 evidence that positive selection occurred in all populations to adapt to their respective environments
165 (the media and the presence of a predator).

166 Parallel evolution events occurred in 32 different genes and eight different promoter regions. Of
167 the 32 genes in which we identified parallel evolution events, 70% could be functionally classified
168 (Figure 2C). Although parallel evolution events arose across and within predator (PE_p) and media
169 (ME_p) evolved populations, both Lines were impacted in different types of genes. A large portion of the
170 parallel mutations that occurred across only ME_p populations were in genes involved in environmental
171 information processing, while the parallel evolution events unique to PE populations were concentrated
172 in genes involved in signaling and cellular processes. Overall, parallel mutations were identified in
173 genes involved in genetic information and processing (PE_p=17%, ME_p=0%, PE_p+ME_p=6%), signaling

174 and cellular processes (PE_p=33%, ME_p=11%, PE_p+ME_p=6%), environmental information processing
175 (PE_p=0%, ME_p=44%, PE_p+ME_p=12%), and metabolism (PE_p=33%, ME_p=11%, and PE_p+ME_p=18%),
176 and unclassified genes (PE_p=17%, ME_p=33%, PE_p+ME_p=59%). Parallel mutations present in only ME
177 or shared between PE and ME populations are likely conferring adaptation to the Neff media, whereas
178 parallel mutations only present in the PE populations suggest that they are important for fitness in the
179 presence of a predator. Since most of the genes in which we identified mutations have not been
180 functionally confirmed in *S. marcescens*, all gene names and predicted functions discussed hereafter
181 must be considered candidate genes/functions.

182 We plotted all the mutations identified in each ME_p and PE_p population and their observed
183 frequencies and found that several parallel mutations were fixed within the populations (Figure 3A).
184 Interestingly, most of the fixed parallel mutations occurred in genes within the same protein-protein
185 interaction network predicted via STRING v12 (48) in close relatives of *S. marcescens*, such as *S.*
186 *rubidaea* and *Yersina enterocolitica* (Figure 3B). This protein network contains the BarA-UvrY two
187 component regulatory system and the three core proteins of the Rcs phosphorelay system, (*rcsC*, *rcsD*,
188 and *rcsB*). Both BarA-UvrY and the Rcs regulatory systems have been shown to play a major role in
189 environmental adaptation and the regulation of virulence in *S. marcescens* (49–51) or related
190 enterobacteria (52–56). Mutations in the histidine kinase *barA* were found in multiple PE_p (3/6) and ME_p
191 populations (5/6), whereas mutations in the response regulator *uvrY* were mostly restricted to ME_p
192 populations (Figure 3C). Mutations in the response regulator of the Rcs system, *rcsB*, were identified at
193 high frequency in virtually all ME_p populations (5/6) but never in the PE_p populations (Figure 3C). One
194 ME_p population (ME_p6) contained a fixed mutation in the transmembrane hybrid kinase *rcsC* and one
195 PE_p population (PE_p3) also had a mutation in *rcsC* but at very low (<10%) frequency (Figure 3C).
196 Within this network, fixed (100 percent frequency) *site-specific* parallel mutations unique to ME_p
197 populations (ME_p2-6) were identified in a promoter region upstream of a gene annotated as the biofilm
198 dispersion protein *bdlA* (Figure 3C). Four of the six PE_p populations (PE_p2, PE_p4, PE_p5, and PE_p6)
199 contained mutations in a gene annotated as the diguanylate cyclase *yfiN*, and of these four populations,
200 three (PE_p4-6) also contained mutations in a promoter upstream of a gene annotated as the outer
201 membrane protein *ompC* (Figure 3C). The genes *bdlA*, *yfiN*, and *ompC* have all been implicated in
202 biofilm formation in other *Enterobacteriaceae* species (57–62). It is important to note that the six PE_p
203 (Lines 1-6) and three ME_p (Lines 1-3) populations were evolved at the same time, but three of the ME_p

204 (Lines 4-6) populations were started over one year later, demonstrating the reproducibility of our
205 results.

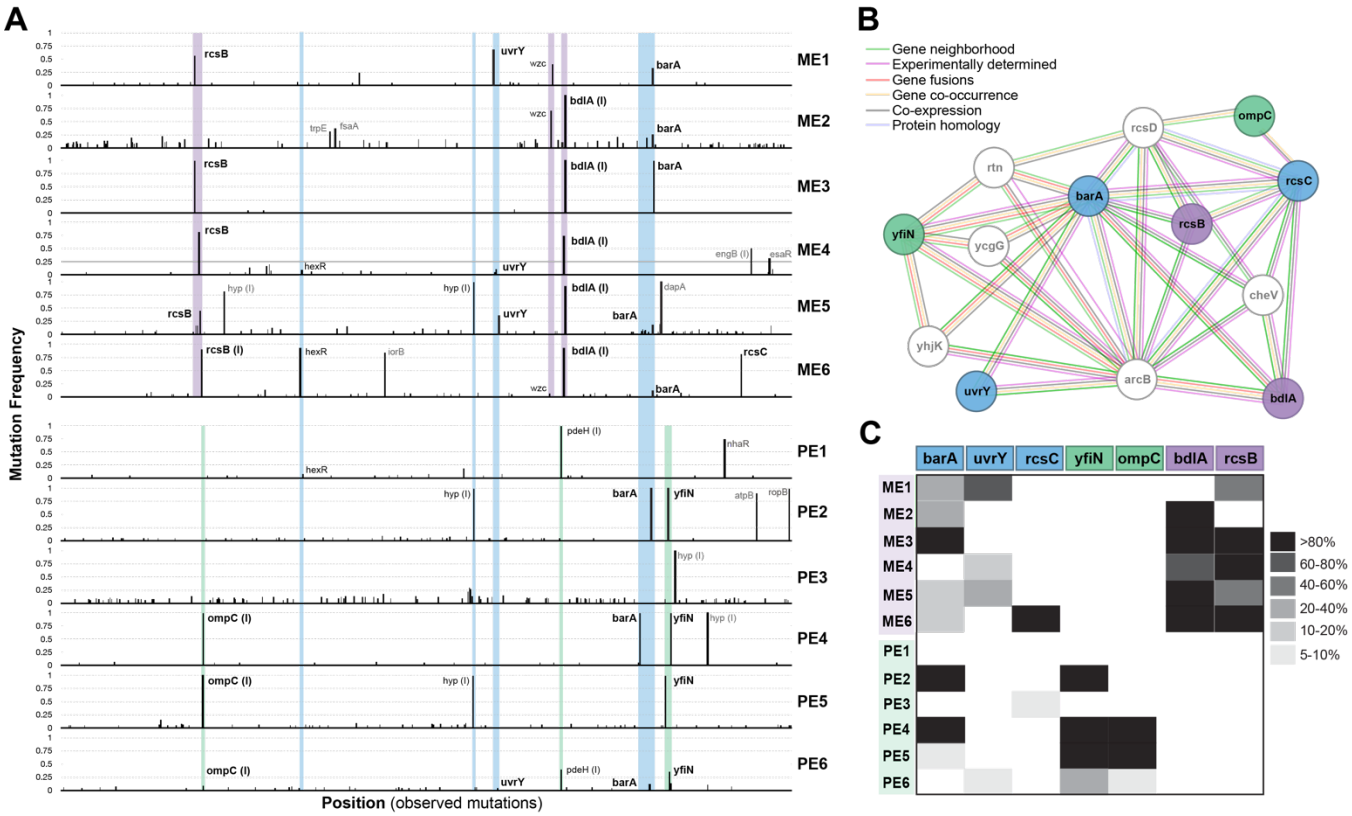

207 **Figure 3.** Frequency of mutations present in the evolved populations. **A)** Plot of all the detected mutations and their
208 frequencies in each population highlighting the parallel and/or "fixed" mutations. Cases of parallel mutation events are
209 highlighted in green (PE only mutations), purple (ME only mutations), and blue (ME-PE). **B)** STRING v12 (48) predicted
210 protein-protein interaction network containing seven genes in which we identified multiple parallel mutations. **C)** Heatmap
211 showing the frequency of mutations in or adjacent (indicated by *) to the seven genes from the same protein-interaction
212 network within each evolved population.

213 *Genotype and phenotype of predator- and media-evolved isolates*

214 To attempt to link specific mutations with phenotypes, a total of three ME_i and six PE_i isolates
215 were sequenced from the evolved populations and compared to the ancestral genome to identify
216 mutations (Figure 4A, Table S2). At least one mutation was detected in each isolate, with a maximum
217 of four and an average of two mutations per isolate (Figure 4A). We identified a total of 24 mutations
218 within or in upstream promoters of 14 genes and 70% of these mutations (17/24) were present at a
219 frequency of >90% in their respective population (Table S2). Additionally, the isolates possessed all the
220 fixed (100% frequency) mutations present within the population from which they were isolated (Figure
221 3A, Supplemental Dataset 1).

222

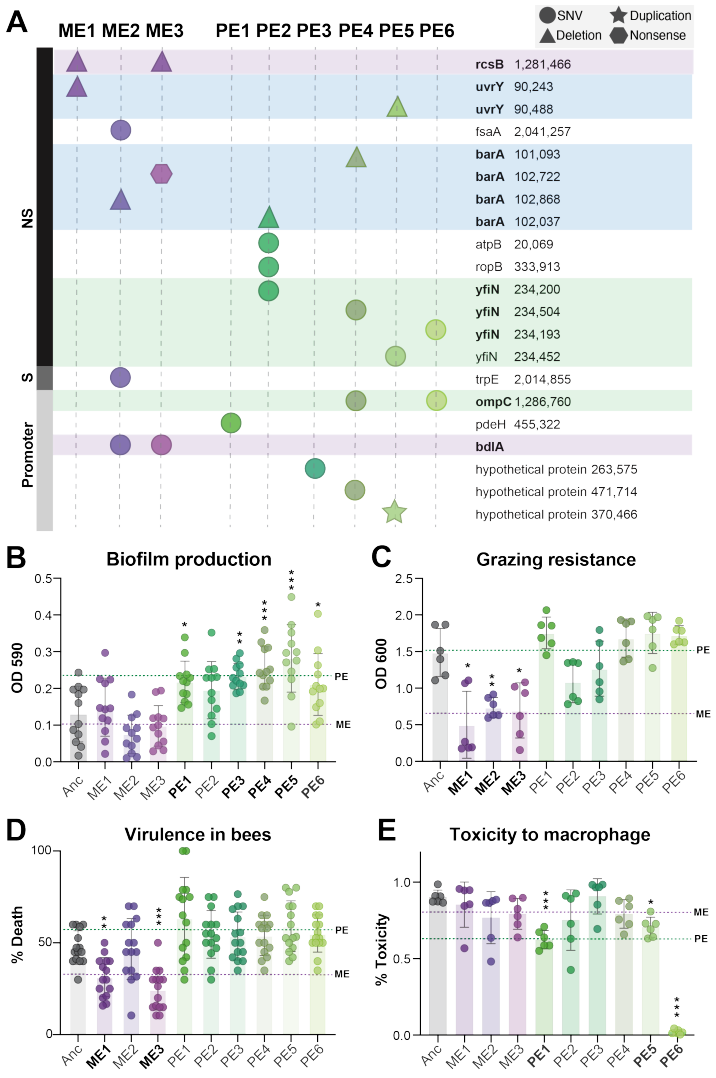

Figure 4. Genotypes and phenotypes of evolved isolates. **A)** Mutations present in each isolate grouped by nonsynonymous (NS), synonymous (S), promoter (intergenic mutation in a promotor region) and indicating the mutation type (single nucleotide variant (SNV), nonsense mutation, duplication, or deletion) and the gene (or gene upstream) affected. **B)** Mean biofilm formation of ME_i and PE_i isolates and the ancestral strain based on 590nm OD readings after 24h of growth in Neff media. Four assays were performed in triplicate and each point represents a biological replicate. **C)** Mean grazing (predation) resistance of PE_i and ME_i isolates and the ancestral strain based on 600nm OD readings of bacterial filtrate after 48h in co-culture with *T. thermophila*. Two assays were performed in triplicate and each point represents a biological replicate. **D)** Percent death of honey bees five days after exposure to the ancestral, ME_i, and PE_i isolates (control group average percent death = 2.3%; see Figure S4). Three replicate assays were performed with five replicates of 20 bees each per isolate per assay (15 replicates total per isolate). Each data point represents a biological replicate of 20 bees. **E)** Percent cytotoxicity of the ancestor, ME_i, and PE_i isolates to murine macrophages (RAW264.7) based on LDH release. **B-E)** Each data point represents a biological replicate (n=6). All box plots show the mean standard deviation. Significance was tested by comparing each evolved isolate to the others and the ancestor using one-way ANOVA with Dunnett's multiple comparisons test. * = P<0.01, **= P<0.001, ***= P<0.0001. Dashed lines represent the overall mean when combining all ME_i (purple line) or PE_i (green line) isolates, respectively.

223 We identified three instances of *site-specific* parallel evolution and three cases of *gene-specific*
224 parallel evolution across the isolates (Figure 4A), all of which occurred within coding regions or
225 promoters upstream of genes within the same BarA-UvrY Rcs protein-protein interaction network
226 (Figure 3B). Two of the three *site-specific* parallel mutations were unique to ME_i isolates: a 66bp
227 deletion in rcsB (ME_i1 and ME_i3) and an intergenic SNV in a promoter upstream of a gene annotated
228 as bdlA (ME_i2 and ME_i3; Figure 4A). The third *site-specific* mutation was unique to PE_i isolates: an
229 intergenic SNV in a promoter upstream of *ompC* (PE_i4 and PE_i6; Figure 4A). Two of the *gene-specific*
230 parallel evolution events occurred in both ME and PE isolates: *barA* (ME_i2, MEv3, PEv2, and PEv4)
231 and *uvrY* (ME_i1 and PE_i5). The third case of *gene-specific* parallel evolution arose in a gene annotated

232 as the inner membrane protein *yfiN* in all PE_i isolates except PE_i1 and PE_i3 (Figure 4A). Overall, most
233 of the mutations present in the isolates likely represent adaptive mutations as they were fixed in their
234 respective populations.

235 To evaluate the phenotypes of the PE_i and ME_i isolates, we performed growth, biofilm
236 production, predation resistance (population size after growth in the presence of *T. thermophila*), and
237 virulence (mortality of honey bees and death of murine macrophage) assays. We chose to specifically
238 analyze isolates, rather than populations, in order to correlate fixed mutations with phenotypic
239 characteristics. To compare growth between the ancestral and evolved strains, we monitored optical
240 density (OD) in spent Neff media (filtered media that had supported *T. thermophila* growth for 48h),
241 fresh Neff media, and LB media every hour for 24 hours. None of the ME_i and PE_i isolates significantly
242 differed in growth in either media type when compared to the ancestor (Figure S2). Because biofilm
243 formation is a strategy for resistance to predation and is also associated with virulence, we measured
244 biofilm production in our ME_i and PE_i isolates compared to the ancestor (Figure 4B). None of the ME_i
245 isolates significantly differed in biofilm production when compared to the ancestor, whereas five of the
246 six PE isolates produced significantly more biofilms than the ancestor (Figure 4B; PE_i1 P=0.017, PE_i3
247 P=0.003, PE_i4 P=0.0001, PE_i5 P<0.0001, PE_i6 P=0.035, one-way ANOVA with Dunnett's multiple
248 comparison test). Overall, when considered together, mean biofilm production of the PE_i isolates was
249 significantly higher than the mean of the ME_i isolates and the ancestor (Figure S3A, P<0.01, with one-
250 way ANOVA with Dunnett's multiple comparison test).

251 In order to determine if exposure to a predator resulted in increased predation resistance, we
252 evaluated grazing resistance (i.e., ability to proliferate in co-culture with a predator) of the ME_i and PE_i
253 isolates. Each isolate was grown with *T. thermophila* for 48h and then the population density of the
254 bacteria was measured. All ME_i isolates were found to be significantly more susceptible to predation
255 than the ancestor (Figure 4C; P< 0.0001, one-way ANOVA with Dunnett's multiple comparison test). In
256 contrast, none of the PE_i isolates significantly differed in resistance to predation relative to the ancestor.
257 However, the mean grazing resistance of all PEi isolates combined was significantly higher than the
258 mean of the ME_i isolates (Figure S3B, P<0.01, with one-way ANOVA with Dunnett's multiple
259 comparison test).

260 We further determined how evolution under predation pressure impacts the virulence of *S.*
261 *marcescens* KZ19 by performing survival assays in a natural host, the honey bee. Honey bees were

262 orally exposed to each individual isolate, the ancestral strain, or sucrose solution only (controls) and
263 monitored every day for five days (Figure S3). We evaluated the percentage of death, five days post-
264 exposure and found that two of the three ME isolates (ME_i1 and ME_i3) displayed significantly
265 attenuated virulence when compared to the ancestral strain (Figure 4D; ME1 P=0.001, ME3 P<0.0001,
266 one-way ANOVA with Dunnett's multiple comparison test). Conversely, none of the PE_i isolates
267 significantly differed from the ancestor in terms of virulence (Figure 4D). Based on probability of survival
268 using a Kaplan-Meier method, we obtained the same results, with only ME_i1 and ME_i3 displaying
269 significantly decreased virulence when compared to the ancestor (Figure S4, P<0.05, Mantel-Cox Log-
270 rank test with Bonferroni correction). However, when comparing the mean percent death five days post-
271 exposure by combining all ME_i and PE_i isolates, the ME_i isolates displayed significant attenuation of
272 virulence when compared to the ancestor and PE_i isolates, and the PE_i isolates were significantly more
273 virulent than the ancestor and the ME_i isolates (Figure 3SC, P<0.01, with one-way ANOVA with
274 Dunnett's multiple comparison test).

275 Several clinical *S. marcescens* isolates have been shown to be cytotoxic to macrophages (63–
276 65). Although *S. marcescens* KZ19 was isolated from the gut of a honey bee, we found that it is
277 capable of killing RAW 264.7 murine macrophages (Figure 4E). Thus, we evaluated the percent of
278 murine macrophage killing by the ancestor and compared it to the ME_i and PE_i isolates based on the
279 release of lactate dehydrogenase (LDH) after two hours of co-culture (MOI 10:1). None of the ME_i
280 isolates differed from the ancestor in terms of cytotoxicity to macrophages. Conversely, three of the PE_i
281 isolates displayed significantly less cytotoxicity to macrophage when compared to the ancestral strain
282 (Figure 4E; PE_i1 P= 0.0009, PE_i5 P=0.03, PE_i6 P<0.0001, one-way ANOVA with Dunnett's multiple
283 comparison test). When all ME_i and PE_i isolates were combined, no difference was observed between
284 the ME_i isolates and the ancestor or the PE_i and ME_i isolates, but the PE_i isolates were significantly less
285 cytotoxic to macrophage cells than the ancestor (Figure 3SD). However, macrophage killing appears to
286 be time and density dependent. In a separate timeseries experiment with a different starting ratio (MOI
287 1:10), we found that all evolved isolates (ME_i and PE_i) displayed overall less cytotoxicity to macrophage
288 than the ancestor at hours 2-5 post exposure, but after six hours they converged in their level of
289 cytotoxicity with all macrophages being killed (lysed) by all isolates and the ancestral strain (Figure S4).
290 Therefore, macrophage cytotoxicity may not be an informative metric for gauging virulence in *S.*
291 *marcescens* KZ19.

292 Finally, we tested whether there was a direct link between pathogenicity in honey bees,
293 cytotoxicity to murine macrophage, biofilm production, and grazing resistance (Figure 5). Despite our
294 relatively small sample size, we found a significant positive correlation between biofilm production and
295 grazing resistance (Figure 5A; r^2=0.56 , P=0.01 , Pearson correlation) as well as between virulence and
296 biofilm production (Figure 5B; r^2=0.5, P=0.02, Pearson correlation) and virulence and grazing
297 resistance (Figure 5C; r^2=0.68, P=0.003, Pearson correlation coefficient). No significant correlations
298 were observed between cytotoxicity to macrophage and any of the other tested phenotypes (Figure 5
299 D-F).

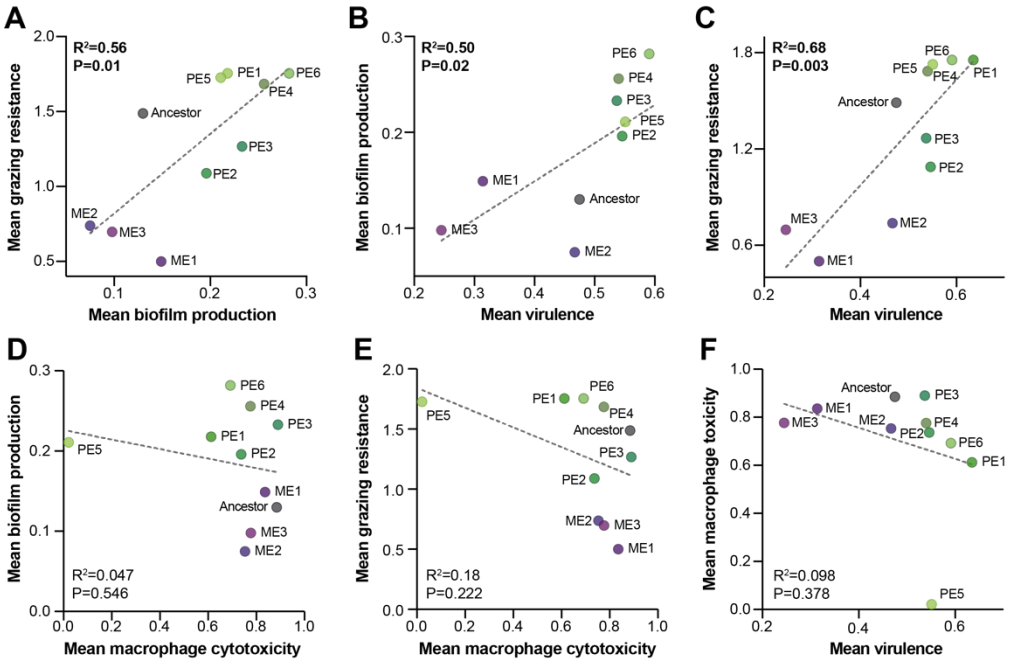

300

301 **Figure 5.** Correlations between mean **A)** biofilm production and grazing resistance, **B)** biofilm production and virulence in
302 bees, **C)** grazing resistance and virulence in bees, **D)** biofilm production and macrophage cytotoxicity, **E)** grazing resistance
303 and macrophage cytotoxicity, and **F)** virulence in bees and macrophage cytotoxicity. Dashed lines represent a simple linear
304 regression, and the correlation strength and significance were tested using the Pearson correlation coefficient.

305

306 **Discussion**

307 Here we revealed that only 60 days of experimental evolution in the presence or absence of a
308 predator resulted in overall consistent genotypic changes in *S. marcescens*, indicated by numerous
309 parallel evolution events. The lower-than-expected number of nonsynonymous mutations coupled with
310 the higher-than-expected number of parallel evolution events suggests that all evolved populations
311 underwent both positive and purifying selection. We also found evidence of positive selection based on

312 the presence of fixed mutations (sweeps) within the same genes, and sometimes in the same exact
313 site, across populations. This is noteworthy as bottlenecks are inherent in experimental evolution and
314 could result in the fixation of random mutations due to drift (66–68). The presence of fixed mutations in
315 the same genes and positions strongly indicate that drift was not the main driver of the sweeps
316 observed in our populations. Although parallel evolution events and sweeps suggest the genes
317 impacted are adaptive, it is possible that some of the observed high frequency mutations are the result
318 of hitchhiking.

319 Despite overall variation in the types of genes impacted, virtually all the fixed mutations within
320 and across PE_p and ME_p populations occurred in genes that are part of the same predicted protein-
321 protein interaction network. Within this protein-protein interaction network, several of the proteins are
322 key components in gene regulatory systems. For example, BarA and UvrY make up a two-component
323 regulatory system (49) and RcsB and RcsC are two of the three major components in the modified two
324 component Rcs phosphorelay system (69), both of which have been shown to regulate the expression
325 of numerous genes in *S. marcescens* (49, 69, 70) and have also been implicated in virulence
326 mechanisms in multiple species of *Enterobacteriaceae* (52–56, 71–73). Thus, mutations in these genes
327 likely have major impacts on multiple other genes by upregulating, downregulating, or stopping
328 expression, resulting in strong selective pressure to maintain beneficial mutations and purge
329 "deleterious" mutations. We hypothesize that mutations that were fixed within one or more genes in this
330 pathway directed the evolutionary trajectories thereafter possibly due to epistatic interactions. However,
331 further studies are needed to validate this hypothesis.
332

333 In order to link specific mutations with phenotypic characteristics, we randomly chose a single
334 isolate from each population. It is important to note that for the ME_p populations we only evaluated
335 isolates from Lines 1-3 because when we originally started this experiment, we only evolved three ME
336 populations. We later realized the importance of having more "control" populations and subsequently
337 evolved three more ME_p Lines, which were only analyzed at the population level in this study. However,
338 we would like to point out that the three ME_p Lines (ME_p4-6) that were evolved over a year after ME_p
339 Lines 1-3 presented mutations in many of the same genes, including several of the fixed mutations that
340 were observed in the first three ME_p populations. This finding underlines the reproducibility of our
341 results and eliminates the probability that contamination could explain the parallel evolution events
342 observed across populations. The genotypic analysis of our three ME_i isolates from Lines 1-3 and six
343 PE_i isolates (one from each evolved population) revealed that all isolates contained the fixed mutations

344 present in their respective population. However, some isolates also contained mutations that were not
345 fixed in the population. Moreover, only two isolates (PE_i1 and PE_i3) contained a single mutation, limiting
346 our ability to directly correlate individual mutations with phenotypes. Based on our results, we predict
347 that the sole mutations present in PE_i1 and PE_i3 in promoter regions upstream of the genes annotated
348 as *pdeH* and a hypothetical protein, respectively, are responsible for the increased biofilm production
349 observed in these two isolates. We also speculate that the large 66bp deletion in *rcsB* present in the
350 ME_i isolates contributed to the attenuated virulence in bees, as seen in ME_i1 and ME_i3 isolates.
351 Furthermore, based on a previous study that demonstrated a role of the BarA-UvrY two component
352 system in controlling the carbon storage regulatory system in *E. coli* (52), it is probable that the
353 mutations we detected in *barA* and *uvrY* in the ME_i and PE_i isolates are the result of adaptation to the
354 Neff media, which contains five percent glucose. We caution that these are only speculations that
355 require further investigation to be validated.

356 The five phenotypes that we evaluated were growth in media, biofilm production, grazing
357 resistance, virulence in honey bees, and cytotoxicity to murine macrophages. We found no change in
358 population density (growth) of any of the isolates when compared to the ancestor in the three media
359 types tested, but we did find changes in biofilm production. Specifically, all PE_i isolates displayed
360 increased biofilm production on average when compared to the ancestor, although PE_i2 was not found
361 to significantly produce more biofilm. The ME_i isolates produced less biofilms than the PE_i and ancestor
362 on average, but individually none of them significantly produced less biofilm than the ancestor. As
363 biofilm production is a natural defense mechanism against predators (74–76), increasing biofilm
364 production could be beneficial in the constant presence of a predator, whereas it is likely not essential
365 in a nutrient rich mono-culture. Although we did not see a significant increase in grazing resistance in
366 any of the PE_i isolates, we did observe a decrease in all three ME_i isolates when compared to the
367 ancestor. It is important to note that in order to maintain *T. thermophia* in co-culture with KZ19 for 24h
368 at the start of the experiment we had to start with a ratio of only 10:1 (bacteria:protist) cell ratio,
369 suggesting the ancestral strain already possessed mechanisms to resist grazing and/or survive
370 phagocytosis. Thus, it is possible that in addition to the pressure to survive predation, competition for
371 resources was a major force impacting the evolution of *S. marcescens* in the presence of *T.*
372 *thermophila* in our experiments. In fact, although we found a strong positive correlation between biofilm
373 production and grazing resistance, increased biofilm formation did appear to increase grazing
374 resistance. Taken together, our results indicate that biofilm production promotes grazing resistance in

375 *S. marcescens* KZ19 but also suggest that increasing biofilm production could be providing other
376 functions in the presence of a predator aside from protection, such as the ability to better compete for
377 resources (77, 78).
378
379 We found that both biofilm production and grazing resistance were positively correlated with
380 virulence in a natural host (the honey bee). The correlation between grazing resistance and bee
381 pathogenicity was particularly strong, especially given our sample size, providing support for the idea
382 that predation can indirectly select for host virulence (5–8). Conversely, we found no correlation
383 between cytotoxicity to murine macrophage cells (RAW 264.7) and biofilm production, grazing
384 resistance, or virulence in bees. In fact, three of the PE isolates were significantly less toxic to
385 macrophage after 2h of exposure, with PE_i5 displaying virtually no cytotoxicity in this assay. Based on
386 our time series experiment, we found that cytotoxicity to RAW 264.7 macrophages is highly time and
387 density dependent. After 6h of co-culture, all isolates and the ancestral strain converged towards high
388 cytotoxicity and had killed all macrophages in the culture. Other strains of *S. marcescens* have been
389 shown to be highly toxic to macrophages (63–65), and our findings confirm this result for *S.*
390 *marcescens* KZ19. However, the lack of correlation between macrophage toxicity and all the other
391 phenotypes we tested suggests that the mutations present in our isolates have no impact on their ability
392 to kill murine macrophage RAW 264.7 cells, and in some rare cases, might render them less toxic.
393 These results indicate that, although evolution in the presence of a predator may increase bacterial
394 virulence, the increase in virulence could be host specific, likely due to the diversity of mechanisms
395 involved in virulence. This underlines the importance of testing the virulence of predator-evolved
396 bacteria in multiple systems.
397 A few other studies have used experimental evolution to directly test how predation by *T.*
398 *thermophila* impacts the virulence of *S. marcescens* (20, 21, 23). Contradictory to our findings, all these
399 studies found that predation attenuated virulence. Some reasons for inconsistencies between our study
400 and previous studies could be due to 1) the use of different *S. marcescens* strains with different life
401 histories, 2) co-evolving *S. marcescens* and *T. thermophila* together (20, 21, 23) rather than preventing
402 the evolution of the predator (this study), 3) using different hosts to test virulence, and 4) differences in
403 the methods used to evaluate virulence. Virulence of the predator-evolved *S. marcescens* in previous
404 studies was evaluated based on either testing entire populations (20) or individual isolates that were
405 then pooled to evaluate virulence (21, 23). By testing a mixture of evolved isolates, it is likely that one
406 will outcompete the others (and that the “winner” will be different depending on the environment).

407 Combining or comparing data from assays performed with different isolates could strongly impact the
408 results since each isolate might genotypically and phenotypically differ (as we observed here) and be
409 more or less fit depending on the context. Moreover, none of these studied evaluated the genotypes of
410 the evolved populations, limiting their ability to fully evaluate how predation impacts the evolution of *S.*
411 *marcescens*. Thus, we believe that the differences in experimental design between the previous
412 predator *S. marcescens* evolution studies and ours likely explains the discrepancy in the results.
413 Fundamentally, our study demonstrates the efficacy of using experimental evolution to identify
414 genes and pathways involved in virulence-associated phenotypes, even over short evolutionary
415 timescales. Despite some variability in the evolutionary outcomes in our experiment, our results provide
416 overall support for the hypotheses (i.e., CEH and the training grounds) that propose bacterial virulence
417 is selected for or maintained by predation. Performing longer evolutionary experiments under different
418 scenarios and with different opportunistic bacterial strains and species will provide a more accurate
419 picture of the forces that drive the evolution of opportunistic pathogens and the mechanisms
420 responsible for their virulence. Identifying virulence mechanisms and understanding how virulence
421 evolves can help guide the development of more effective treatment strategies for combating bacterial
422 infections.
423

424 **Materials and Methods**

425 *Grazing confirmation*

426 To confirm that *T. thermophila* grazes on *S. marcescens* KZ19, we utilized transconjugant KZ19
427 containing an E2 crimson fluorescent protein with spectinomycin resistance (38, 43). The
428 transconjugant KZ19 strain was inoculated into 3mL of LB broth containing 180ug/mL spectinomycin
429 and incubated at 30°C for 24h. After 24h, 1OD of the transconjugant KZ19 was resuspended in fresh
430 Neff media and 1mL was pipetted into 3mL of Neff media containing *T. thermophila* and 180ug/mL
431 spectinomycin. The culture was incubated for 24h at 30°C. One mL of the 24h co-culture was then
432 centrifuged at 2000g for 10m to collect the *T. thermophila* cells, the supernatant containing bacteria
433 was discarded, and the *T. thermophila* were resuspended in 1mL of axenic Neff media. The *T.*
434 *thermophila* cells were then pipetted onto a microscope slide that was washed with 60% EtOH (which
435 immobilizes the cells without immediately lysing them), covered with a glass cover slip, and imaged on
436 a Keyence BZ-X700 Series All-In-One Fluorescence Microscope in brightfield and with a Cy5 filter.

437 *Experimental evolution*

438 *Serratia marcescens* strain KZ19 was evolved either in media alone (media-evolved) or with the
439 predator *T. thermophila* strain SB210 (predator-evolved). *T. thermophila* strain SB210 was purchased
440 from the Tetrayhema Stock Center located at Cornell University. The media-evolved (ME) experiment
441 included three replicate Lines and the predator-evolved (PE) experiment included six replicate Lines.
442 First, *T. thermophila* and the ancestral *S. marcescens* KZ19 were cultured individually for 72h and 24h,
443 respectively, at 30°C in Neff media. To start each evolved Line, 1OD of the overnight KZ19 culture was
444 resuspended in fresh Neff media and 1mL was added to either 3mL of Neff media alone (ME_p Lines) or
445 3mL Neff media containing *T. thermophila* culture (PE_p Lines) at a ratio of 10:1 cells
446 (bacteria:protist).The starting ratio of *S. marcescens*:*T. thermophila* was based on preliminary trials
447 starting with various concentrations of *S. marcescens* and *T. thermophila* co-inoculated in Neff media to
448 determine the ratio that would allow both organisms to remain in co-culture for 24h.

449 The 3mL experimental cultures were incubated at 30°C without shaking. Every 24h for 60 days
450 the cultures were vortexed and 1% of each culture was sampled from the flasks and added to 3mL of
451 either 1) fresh Neff media or 2) new axenic cultures of *T. thermophila* in Neff media. Every day, prior to
452 passaging, the cultures were checked for *T. thermophila* viability and density via microscopy and the
453 successful passaging and growth of *S. marcescens* presence was evaluated by plating on Luria-Bertani
454 (LB) agar. Every day over the course of the 60-day evolution experiment, *T. thermophila* and *S.*
455 *marcescens* were always detected. Although population size was not directly measured at every
456 passage, based on daily plating (*S. marcescens*) and light microscopy (*T. thermophila*), we never
457 observed a noticeable difference in population size. The number of generations reached for each *S.*
458 *marcescens* evolved population over the course of 60 days is estimated to be approximately 396.

459 On day 60, six LB agar plates were streak inoculated from the culture flasks and incubated for
460 24h at 30°C. One bacterial colony was randomly selected from each of the six the PE populations
461 (PE1-6) and three of the ME populations (ME1-3).Pure cultures of each isolate were created by
462 inoculating in 3mL LB broth with 24h incubation at 30°C. Samples (200 µL from each pure culture) were
463 then frozen at -80°C in 20% glycerol. These nine isolates were sequenced, analyzed, and used for
464 phenotypic analysis (i.e., virulence in bees, growth in media, biofilm production, macrophage
465 cytotoxicity, and grazing resistance).

466 *DNA Extraction and Sequencing*

467 Cultures of the evolved populations (ME n=6, PE n=6), evolved isolates (ME n=3, PE n=6) and the
468 ancestor were diluted to 1 OD. DNA extractions were performed using the Zymo Quick-DNA
469 Fungal/Bacterial Miniprep Kit (D6005). DNA was prepped for sequencing using the Oxford Nanopore
470 Rapid Barcoding Sequencing gDNA Kit (SQK-RBK004) for long read sequencing and the Illumina
471 Nextera DNA Flex Library Prep Kit (20018704) for short read sequencing. The ancestral genome was
472 sequenced via long (Oxford Nanopore Minion) and short (Illumina iSeq100) read technologies. The
473 evolved populations and isolates were sequenced via short read technology on an Illumina iSeq100
474 with 2x150 paired end reads. See Table S1 for sequencing depth details.

475 *Genome Assembly and Analysis*

476 The Illumina and Nanopore reads of the ancestral genome were then used to generate a hybrid
477 assembly using hybridSPAdes v3.15.3 (79). Assembled scaffolds were annotated using Prokka v1.14.5
478 (80) on the Department of Energy Systems Biology Knowledgebase (KBase) platform (81). We also
479 mapped all short reads of the ancestral strain back to the consensus ancestral genome using BreSeq
480 v0.38.1 (45). Any mutations predicted by BreSeq when the ancestral reads were mapped to the
481 ancestral consensus genome were considered sequencing or assembly issues in the ancestral genome
482 and removed as candidate mutations in the evolved populations and isolates.

483 The sequencing reads of the evolved populations and isolates were trimmed using Trimmomatic
484 v0.40 (82). The trimmed reads were then mapped to the newly assembled ancestral genome using
485 BreSeq v0.37.0 (45) with a base-quality-cutoff PHRED score of 30 and minimum frequency cutoff of
486 0.05 to identify mutations. Promoters were predicted using iProEP (83). Functional characterization of
487 genes (Figure 2- Table Supplement 2) was predicted using KOALA KEGG Orthology And Links
488 Annotation (46, 84). Protein-protein interaction network prediction was determined using the STRING
489 v12 database (48) using *S. marcescens*, *S. rubidaea* and *Y. enterocolitica* as reference organisms.
490 Simulations to determine the percent mutations expected at random across intergenic, synonymous
491 and non-synonymous positions and the probability of *gene-* and *site-specific* parallel mutations based
492 on random expectation were conducted with a custom Python script: we conducted 10,000 independent
493 simulations where one mutation was introduced at random under a Jukes & Cantor model in the
494 reference genome of *S. marcescens* KZ19 (GCA_002915435.1). The annotations of the genome were
495 used to infer whether the mutation was intergenic or not. Mutations affecting coding sequences were
496 inferred as synonymous or non-synonymous by translating the gene *in silico* before and after
497 introducing the mutation.

498 *Growth assay*

499 Growth assays were performed in triplicate in both LB broth, fresh Neff media, and spent Neff media
500 with *T. thermophila* filtered out (i.e., *T. thermophila* were grown in the media for 48h before filtering).
501 Pure 1OD cultures of the evolved isolates and the ancestor were diluted to 10^{-5} and 5µL of the culture
502 was pipetted into 200µL of media in a 96-well microplate. Absorbance detection was performed at an
503 OD of 600nm at 30°C with shaking every hour for 24h on a BioTek Synergy™ 2 plate reader.

504 *Biofilm assay*

505 Biofilm assays were performed in triplicate for each isolate. Pure 1OD cultures of the evolved isolates
506 and the ancestor were diluted to 10^{-5} and 5µL of the culture was pipetted into 200µL of media in a 96-
507 well microplate. The covered plate was incubated for 36h at 30°C without shaking. After 36h, the
508 supernatant was poured off, the wells were washed twice with 200µL of sterile ddH_2O, and the cells
509 were stained with 150µL of 0.04% crystal violet for 10 minutes. After 10 minutes, the excess crystal
510 violet was removed, the wells were washed again and stained once more for 10 minutes. The crystal
511 violet was poured off and cells were solubilized with 150µL of 95% ethanol. OD readings were taken at
512 absorbance reading 560nm on the BioTek Synergy™ 2 plate reader. A total of four assays were
513 performed, each in triplicate.

514 *Grazing resistance assay*

515 Grazing resistance assays were performed in triplicate for each isolate. Cultures of the evolved isolates
516 and the ancestor were grown overnight, normalized the 1OD, and 1mL was added to a culture flask
517 containing *T. thermophila* in 3mL Neff media (10:1 ration of bacteria to protist cells). *T. thermophila*
518 alone in 3mL Neff media served as the negative control. Experimental culture flasks were incubated at
519 30°C for 48h. After 48h, the cultures were mixed thoroughly and 1mL was sampled and centrifuged at
520 5,000 rpm for 10 minutes. The supernatant was discarded, pellets were resuspended in 1mL 1X PBS,
521 and the solution was filtered through 5.0 µm MilliporeSigma™ Millex™-SV Sterile PVDF syringe filters
522 to remove the *T. thermophila* cells. OD readings were taken of filtrates at 600nm after blanking with the
523 negative control filtrate. A total of two assays were performed, each in triplicate.

524 *Virulence assay*

525 Pure 1OD cultures of the evolved isolates and the ancestor were pelleted via centrifugation and
526 resuspended in a 1:1 sterile sugar syrup solution (SSS). Conventional adult honey bee workers (*Apis*

527 *mellifera*) were sampled from a single hive located on the Gateway North Research Campus in Browns
528 Summit, North Carolina. Bees were immobilized at 4°C, randomly distributed into groups, and exposed
529 via the immersion method (38) to ~10 µL of one of three treatments: 1) sterile SSS only, 2) the ancestor
530 in sterile SSS, or 3) each evolved isolate in sterile SSS. Bees were kept in cup cages (20 bees/cup;
531 100 bees/treatment) under hive conditions: 35°C and 95% humidity. Mortality between the treatments
532 was noted every day for 5 days. A total of three assays were performed with five replicates per assay
533 equaling 300 bees tested in total per isolate. A survival curve (Kaplan-Meier) was created in GraphPad
534 Prism v9.1.0.

535 *Macrophage cytotoxicity assay*

536 Murine macrophage cells (Raw 264.7) were maintained in Dulbecco's Modified Eagle's Medium
537 (DMEM, ATCC: 30-2002) with 10% Fetal Bovine Serum (FBS, ATCC: 30-2020) at 37°C with 5% CO_2.
538 After reaching 90% confluency, cells were harvested, resuspended in 500uL of DMEM media in a
539 Corning™ Costar™ 24-well Clear TC-treated well plate (Fisher Scientific: 09-761-146), and incubated
540 overnight at 37°C with 5% CO_2. After overnight incubation, the old DMEM media was discarded, the
541 macrophage cells were washed with 1X PBS, and 500µL of fresh DMEM media was added to each
542 well. Overnight cultures of each bacterial isolate were normalized to 1 OD prior to the experiment and
543 ten microliters of each 1 OD bacterial culture (MOI 10:1) was added into a separate well containing
544 macrophage and incubated at 37°C with 5% CO_2. For control wells (macrophage spontaneous
545 release), 10µL of 1X PBS was added instead of bacteria. The cytotoxicity was measured after two
546 hours using the CytoTox 96® Non-Radioactive Cytotoxicity Assay. In brief, two hours after co-culturing,
547 the media from each well (including controls) was mixed two times and 60µL was pipetted into a 1.7mL
548 tube and centrifuged at 10,000 rpm for two minutes to pellet bacterial cells. After centrifuging, 50µL of
549 the supernatant was transferred into a new 96-well plate (Fisher Scientific: 07-200-90) to measure
550 lactate dehydrogenase (LDH) release (OD_{490}). For control wells, the macrophage lysis buffer release
551 was measured by adding 50µL 10X lysis buffer to macrophage samples 45 minutes prior to LDH
552 measurement, and the negative control was measured without adding lysis buffer. The percent
553 cytotoxicity was calculated using the equation below. The ratio of 55/51 was used to correct the volume
554 change caused by the lysis buffer. A single assay was performed with six replicates.

555

556 $$Percent\ cytotoxicity = 100 \times \frac{Experimental\ treatment\ release - mean\ (macrophage\ spontaneous\ release)}{\frac{55}{51}(mean(macrophage\ lysis\ buffer\ Release) - mean\ (macrophage\ spontaneous\ release))}$$

557

558 Since virtually all isolates were highly cytotoxic to macrophage after two hours at MOI of 10:1
559 cells (bacteria:macrophage), we performed a time series experiment to determine if macrophage
560 cytotoxicity is time and density dependent. The Raw 264.7 macrophages and bacterial cultures were
561 prepared as described above, except this time the assay started with a ratio of 1:10 (MOI) bacteria to
562 macrophage cells and cytotoxicity via LDH release (CytoTox 96® Non-Radioactive Cytotoxicity Assay)
563 was measured at five timepoints following co-culture (2h, 3h, 4h, 5h, and 6h). Cytotoxicity in this assay
564 was based on optical density at OD490 rather than percent cytotoxicity. At 6h, all macrophages co-
565 cultured with the ancestral and evolved isolates were dead as indicated by cell lysis observed under an
566 inverted light microscope. One assay was performed in triplicate.

567 *Materials availability*

568 All raw sequencing data has been deposited on NCBI under BioProject PRJNA838621.

569 **Acknowledgments**
570 We would like to thank Dr. Carlos Goller for assistance with the Nanopore sequencing. We also want to
571 thank Dr. Louis-Marie Bobay for helping with the simulations and providing constructive and helpful
572 feedback on the manuscript. This work was supported by the National Science Foundation under grant
573 DEB- 2344788 (to K.R.), the National Institutes of Health under grant 7R01GM145747-02 (to K.R.), the
574 University of North Carolina Greensboro (UNCG) College of Arts and Sciences Faculty First Award (to
575 K.R.), and UNCG Department of Biology Graduate Student Support grants (to H.A.H and C.L.).

576

577 **Author Contributions**

578 H.A.H., C.L. and M-J.L. performed the experiments and collected the data. K.R. designed and funded
579 the research. All authors contributed data analysis and manuscript writing and editing.

580 **Competing Interest Statement**

581 The authors declare no competing interests.

582

583 **References**

584 1. Brown SP, Cornforth DM, Mideo N. 2012. Evolution of virulence in opportunistic pathogens:
585 generalism, plasticity, and control. Trends in Microbiology 20:336–342.

586 2. Sokurenko EV, Gomulkiewicz R, Dykhuizen DE. 2006. Source–sink dynamics of virulence
587 evolution. Nat Rev Microbiol 4:548–555.

588 3. Pandey A, Mideo N, Platt TG. 2022. Virulence evolution of pathogens that can grow in reservoir
589 environments. The American Naturalist 199:141–158.

590 4. Casadevall A, Pirofski L. 2007. Accidental virulence, cryptic pathogenesis, martians, lost hosts,
591 and the pathogenicity of environmental microbes. Eukaryot Cell 6:2169–2174.

592 5. Levin BR, Edén CS. 1990. Selection and evolution of virulence in bacteria: an ecumenical
593 excursion and modest suggestion. Parasitology 100:S103–S115.

594 6. Levin B. 1996. The evolution and maintenance of virulence in microparasites. Emerg Infect Dis
595 2:93–102.

596 7. Barker J, Brown MR. 1994. Trojan horses of the microbial world: protozoa and the survival of
597 bacterial pathogens in the environment. Microbiology 140 (Pt 6):1253–1259.

598 8. Molmeret M, Horn M, Wagner M, Santic M, Abu Kwaik Y. 2005. Amoebae as training grounds for
599 intracellular bacterial pathogens. Appl Environ Microbiol 71:20–28.

600 9. Erken M, Lutz C, McDougald D. 2013. The rise of pathogens: Predation as a factor driving the
601 evolution of human pathogens in the environment. Microb Ecol 65:860–868.

602 10. Amaro F, Martín-González A. 2021. Microbial warfare in the wild—the impact of protists on the
603 evolution and virulence of bacterial pathogens. Int Microbiol 24:559–571.

604 11. Cirillo JD, Cirillo SLG, Yan L, Bermudez LE, Falkow S, Tompkins LS. 1999. Intracellular growth in
605 *Acanthamoeba castellanii* affects monocyte entry mechanisms and enhances virulence of
606 *Legionella pneumophila*. Infect Immun 67:4427–4434.

607 12. Rasmussen MA, Carlson SA, Franklin SK, McCuddin ZP, Wu MT, Sharma VK. 2005. Exposure to
608 rumen protozoa leads to enhancement of pathogenicity of and invasion by multiple-antibiotic-
609 resistant *Salmonella enterica* Bearing SGI1. Infect Immun 73:4668–4675.

610 13. Adiba S, Nizak C, van Baalen M, Denamur E, Depaulis F. 2010. From grazing resistance to
611 pathogenesis: The coincidental evolution of virulence factors. PLoS ONE 5:e11882.

612 14. Coombes BK, Gilmour MW, Goodman CD. 2011. The evolution of virulence in non-O157 Shiga
613 toxin-producing Escherichia coli. Front Microbio 2.

614 15. Rehfuss MYM, Parker CT, Brandl MT. 2011. Salmonella transcriptional signature in Tetrahymena
615 phagosomes and role of acid tolerance in passage through the protist. ISME J 5:262–273.

616 16. Hosseinidoust Z, van de Ven TGM, Tufenkji N. 2013. Evolution of Pseudomonas aeruginosa
617 virulence as a result of phage predation. Appl Environ Microbiol 79:6110–6116.

618 17. Lenski RE. 2017. Experimental evolution and the dynamics of adaptation and genome evolution in
619 microbial populations. ISME J 11:2181–2194.

620 18. Cooper VS. 2018. Experimental evolution as a high-throughput screen for genetic adaptations.
621 mSphere 3:e00121-18.

622 19. McDonald MJ. 2019. Microbial experimental evolution – a proving ground for evolutionary theory
623 and a tool for discovery. EMBO Rep 20:e46992.

624 20. Friman V-P, Lindstedt C, Hiltunen T, Laakso J, Mappes J. 2009. Predation on multiple trophic
625 levels shapes the evolution of pathogen virulence. PLoS ONE 4:e6761.

626 21. Mikonranta L, Friman V-P, Laakso J. 2012. Life history trade-offs and relaxed selection can
627 decrease bacterial virulence in environmental reservoirs. PLoS ONE 7:e43801.

628 22. Friman V-P, Buckling A. 2014. Phages can constrain protist predation-driven attenuation of
629 Pseudomonas aeruginosa virulence in multienemy communities. ISME J 8:1820–1830.

630 23. Zhang J, Ketola T, Örmälä-Odegrip A-M, Mappes J, Laakso J. 2014. Coincidental loss of bacterial
631 virulence in multi-enemy microbial communities. PLoS ONE 9:e111871.

632 24. Leong W, Poh WH, Williams J, Lutz C, Hoque MM, Poh YH, Yee BYK, Chua C, Givskov M,
633 Sanderson-Smith M, Rice SA, McDougald D. 2022. Adaptation to an amoeba host leads to
634 Pseudomonas aeruginosa isolates with attenuated virulence. Appl Environ Microbiol 88:e02322-
635 21.

636 25. Hoque MM, Noorian P, Espinoza-Vergara G, Manuneedhi Cholan P, Kim M, Rahman MH,
637 Labbate M, Rice SA, Pernice M, Oehlers SH, McDougald D. 2022. Adaptation to an amoeba host
638 drives selection of virulence-associated traits in Vibrio cholerae. ISME J 16:856–867.

639 26. Nair RR, Vasse M, Wielgoss S, Sun L, Yu Y-TN, Velicer GJ. 2019. Bacterial predator-prey
640 coevolution accelerates genome evolution and selects on virulence-associated prey defences. Nat
641 Commun 10:4301.

642 27. Santos-Lopez A, Marshall CW, Scribner MR, Snyder DJ, Cooper VS. Evolutionary pathways to
643 antibiotic resistance are dependent upon environmental structure and bacterial lifestyle. eLife
644 8:e47612.

645 28. Santos-Lopez A, Marshall CW, Haas AL, Turner C, Rasero J, Cooper VS. 2021. The roles of
646 history, chance, and natural selection in the evolution of antibiotic resistance. eLife 10:e70676.

647 29. Rodríguez-Verdugo A, Carrillo-Cisneros D, González-González A, Gaut BS, Bennett AF. 2014.
648 Different tradeoffs result from alternate genetic adaptations to a common environment.
649 Proceedings of the National Academy of Sciences 111:12121–12126.

650 30. Tenaillon O, Rodríguez-Verdugo A, Gaut RL, McDonald P, Bennett AF, Long AD, Gaut BS. 2012.
651 The molecular diversity of adaptive convergence. Science 335:457–461.

652 31. Blount ZD, Borland CZ, Lenski RE. 2008. Historical contingency and the evolution of a key
653 innovation in an experimental population of Escherichia coli. Proc Natl Acad Sci U S A 105:7899–
654 7906.

655 32. Grimont PAD, Grimont F. 1978. The genus Serratia. Annu Rev Microbiol 32:221–248.

656 33. Almuneef MA, Baltimore RS, Farrel PA, Reagan-Cirincione P, Dembry LM. 2001. Molecular typing
657 demonstrating transmission of gram-negative rods in a neonatal intensive care unit in the absence
658 of a recognized epidemic. Clinical Infectious Diseases 32:220–227.

659 34. Ochieng JB, Boisen N, Lindsay B, Santiago A, Ouma C, Ombok M, Fields B, Stine OC, Nataro JP.
660 2014. *Serratia marcescens* is injurious to intestinal epithelial cells. Gut Microbes 5:729–736.

661 35. Hejazi A, Falkiner FR. 1997. Serratia marcescens. Journal of Medical Microbiology 46:903–912.

662 36. Khanna A. 2013. Serratia Marcescens - A rare opportunistic nosocomial pathogen and measures
663 to limit its spread in hospitalized patients. JCDR https://doi.org/10.7860/JCDR/2013/5010.2737.

664 37. Montagnani C, Cocchi P, Lega L, Campana S, Biermann KP, Braggion C, Pecile P, Chiappini E,
665 de Martino M, Galli L. 2015. Serratia marcescens outbreak in a neonatal intensive care unit:
666 crucial role of implementing hand hygiene among external consultants. BMC Infectious Diseases
667 15:11.

668 38. Raymann K, Coon KL, Shaffer Z, Salisbury S, Moran NA. 2018. Pathogenicity of Serratia
669 marcescens strains in honey bees. mBio 9.

670 39. Raymann K, Shaffer Z, Moran NA. 2017. Antibiotic exposure perturbs the gut microbiota and
671 elevates mortality in honeybees. PLoS Biol 15:e2001861.

672 40. Motta EVS, Raymann K, Moran NA. 2018. Glyphosate perturbs the gut microbiota of honey bees.
673 Proc Natl Acad Sci USA 115:10305–10310.

674 41. Steele MI, Motta EVS, Gattu T, Martinez D, Moran NA. 2021. The gut microbiota protects bees
675 from invasion by a bacterial pathogen. Microbiol Spectr 9:e00394-21.

676 42. Powell JE, Carver Z, Leonard SP, Moran NA. 2021. Field-realistic tylosin exposure impacts honey
677 bee microbiota and pathogen susceptibility, Which Is Ameliorated by Native Gut Probiotics.
678 Microbiol Spectr 9.

679 43. Leonard SP, Perutka J, Powell JE, Geng P, Richhart DD, Byrom M, Kar S, Davies BW, Ellington
680 AD, Moran NA, Barrick JE. 2018. Genetic engineering of bee gut microbiome bacteria with a
681 toolkit for modular assembly of broad-host-range plasmids. ACS Synth Biol 7:1279–1290.

682 44. Bankevich A, Nurk S, Antipov D, Gurevich AA, Dvorkin M, Kulikov AS, Lesin VM, Nikolenko SI,
683 Pham S, Prjibelski AD, Pyshkin AV, Sirotkin AV, Vyahhi N, Tesler G, Alekseyev MA, Pevzner PA.
684 SPAdes: a new genome assembly algorithm and its applications to single-cell sequencing. J
685 Comput Biol. 2012 May;19(5):455-77.

686 45. Deatherage DE, Barrick JE. 2014. Identification of mutations in laboratory-evolved microbes from
687 next-generation sequencing data using breseq, p. 165–188. *In* Sun, L, Shou, W (eds.),
688 Engineering and Analyzing Multicellular Systems. Springer New York, New York, NY.

689 46. Kanehisa M, Goto S. 2000. KEGG: kyoto encyclopedia of genes and genomes. Nucleic Acids Res
690 28:27–30.

691 47. Jukes T. H., Cantor C. R. 1969. Evolution of protein molecules, in Mammalian Protein Metabolism.
692 New York, NY: Academic Press, 21–132

693 48. Szklarczyk D, Kirsch R, Koutrouli M, Nastou K, Mehryary F, Hachilif R, Gable AL, Fang T,
694 Doncheva NT, Pyysalo S, Bork P, Jensen LJ, von Mering C. 2023. The STRING database in
695 2023: protein-protein association networks and functional enrichment analyses for any sequenced
696 genome of interest. Nucleic Acids Res 51:D638–D646.

697 49. Liu X, Xu D, Wu D, Xu M, Wang Y, Wang W, Ran T. 2023. BarA/UvrY differentially regulates
698 prodigiosin biosynthesis and swarming motility in Serratia marcescens FS14. Res Microbiol
699 174:104010.

700 50. Romanowski EG, Stella NA, Romanowski JE, Yates KA, Dhaliwal DK, St. Leger AJ, Shanks RMQ.
701 The Rcs stress response system regulator GumB modulates Serratia marcescens-induced

702 inflammation and bacterial proliferation in a rabbit keratitis model and cytotoxicity in vitro. Infect
703 Immun 89:e00111-21.

704 51. Di Venanzio G, Stepanenko TM, García Véscovi E. 2014. Serratia marcescens ShlA pore-forming
705 toxin is responsible for early induction of autophagy in host cells and is transcriptionally regulated
706 by RcsB. Infect Immun 82:3542–3554.

707 52. Pernestig A-K, Georgellis D, Romeo T, Suzuki K, Tomenius H, Normark S, Melefors Ö. 2003. The
708 *Escherichia coli* BarA-UvrY two-component system is needed for efficient switching between
709 glycolytic and gluconeogenic carbon sources. J Bacteriol 185:843–853.

710 53. Teplitski M, Goodier RI, Ahmer BMM. 2003. Pathways leading from BarA/SirA to motility and
711 virulence gene expression in *Salmonella*. J Bacteriol 185:7257–7265.

712 54. Herren CD, Mitra A, Palaniyandi SK, Coleman A, Elankumaran S, Mukhopadhyay S. 2006. The
713 BarA-UvrY two-component system regulates virulence in avian pathogenic *Escherichia coli*
714 O78:K80:H9. Infect Immun 74:4900–4909.

715 55. Palaniyandi S, Mitra A, Herren CD, Lockatell CV, Johnson DE, Zhu X, Mukhopadhyay S. 2012.
716 BarA-UvrY two-component system regulates virulence of uropathogenic E. coli CFT073. PLoS
717 One 7:e31348.

718 56. Tomenius H, Pernestig A-K, Jonas K, Georgellis D, Möllby R, Normark S, Melefors Ö. 2006. The
719 Escherichia coli BarA-UvrY two-component system is a virulence determinant in the urinary tract.
720 BMC Microbiol 6:27.

721 57. Katharios-Lanwermeyer S, Koval SA, Barrack KE, O'Toole GA. The diguanylate cyclase yfiN of
722 Pseudomonas aeruginosa regulates biofilm maintenance in response to peroxide. J Bacteriol
723 204:e00396-21.

724 58. Sanchez-Torres V, Hu H, Wood TK. 2011. GGDEF proteins YeaI, YedQ, and YfiN reduce early
725 biofilm formation and swimming motility in Escherichia coli. Appl Microbiol Biotechnol 90:651–658.

726 59. Huertas MG, Zárate L, Acosta IC, Posada L, Cruz DP, Lozano M, Zambrano MM. 2014. Klebsiella
727 pneumoniae yfiRNB operon affects biofilm formation, polysaccharide production and drug
728 susceptibility. Microbiology (Reading) 160:2595–2606.

729 60. Morgan R, Kohn S, Hwang S-H, Hassett DJ, Sauer K. 2006. BdlA, a chemotaxis regulator
730 essential for biofilm dispersion in Pseudomonas aeruginosa. J Bacteriol 188:7335–7343.

731 61. Petrova OE, Sauer K. 2012. Dispersion by Pseudomonas aeruginosa requires an unusual
732 posttranslational modification of BdlA. Proceedings of the National Academy of Sciences
733 109:16690–16695.

734 62. Yeom J, Lee Y, Park W. 2012. Effects of non-ionic solute stresses on biofilm formation and
735 lipopolysaccharide production in *Escherichia coli* O157:H7. Research in Microbiology 163:258–
736 267.

737 63. Ishii K, Adachi T, Imamura K, Takano S, Usui K, Suzuki K, Hamamoto H, Watanabe T, Sekimizu
738 K. 2012. Serratia marcescens induces apoptotic cell death in host immune cells via a
739 lipopolysaccharide- and flagella-dependent mechanism. J Biol Chem 287:36582–36592.

740 64. Krzymińska S, Ochocka K, Kaznowski A. 2012. Apoptosis of epithelial cells and macrophages due
741 to nonpigmented Serratia marcescens strains. ScientificWorldJournal 2012:679639.

742 65. Krzymińska S, Raczkowska M, Kaznowski A. 2010. Cytotoxic activity of Serratia marcescens
743 clinical isolates. Pol J Microbiol 59:201–205.

744 66. Gamblin J, Gandon S, Blanquart F, Lambert A. 2023. Bottlenecks can constrain and channel
745 evolutionary paths. Genetics 224:iyad001.

746 67. Mahrt N, Tietze A, Künzel S, Franzenburg S, Barbosa C, Jansen G, Schulenburg H. 2021.
747 Bottleneck size and selection level reproducibly impact evolution of antibiotic resistance. 9. Nat
748 Ecol Evol 5:1233–1242.

749 68. Wahl LM, Gerrish PJ, Saika-Voivod I. 2002. Evaluating the impact of population bottlenecks in
750 experimental evolution. Genetics 162:961–971.

751 69. Pan X, Tang M, You J, Liu F, Sun C, Osire T, Fu W, Yi G, Yang T, Yang S-T, Rao Z. 2021.
752 Regulator RcsB controls prodigiosin synthesis and various cellular processes in Serratia
753 marcescens JNB5-1. Appl Environ Microbiol 87:e02052-20.

754 70. Trouillon J, Attrée I, Elsen S. 2023. The regulation of bacterial two-partner secretion systems.
755 Molecular Microbiology 120:159–177.

756 71. Meng J, Young G, Chen J. 2021. The Rcs System in Enterobacteriaceae: Envelope stress
757 responses and virulence regulation. Front Microbiol 12:627104.

758 72. Heeb S, Haas D. 2001. Regulatory roles of the GacS/GacA two-component system in plant-
759 associated and other gram-negative bacteria. Mol Plant Microbe Interact 14:1351–1363.

760 73. Huang Y-H, Ferrières L, Clarke DJ. 2006. The role of the Rcs phosphorelay in
761 Enterobacteriaceae. Res Microbiol 157:206–212.

762 74. Flemming H-C, Wingender J. 2010. The biofilm matrix. Nat Rev Microbiol 8:623–633.

763 75. Hoque MM, Espinoza-Vergara G, McDougald D. 2023. Protozoan predation as a driver of diversity
764 and virulence in bacterial biofilms. FEMS Microbiol Rev 47:fuad040.

765 76. Wucher BR, Elsayed M, Adelman JS, Kadouri DE, Nadell CD. 2021. Bacterial predation
766 transforms the landscape and community assembly of biofilms. Curr Biol 31:2643-2651.e3.

767 77. Oliveira NM, Martinez-Garcia E, Xavier J, Durham WM, Kolter R, Kim W, Foster KR. 2015. Biofilm
768 formation as a response to ecological competition. PLoS Biol 13:e1002191.

769 78. Rendueles O, Ghigo J-M. 2015. Mechanisms of competition in biofilm communities. Microbiol
770 Spectrum 3:10.1128/microbiolspec.mb-0009–2014.

771 79. Antipov D, Korobeynikov A, McLean JS, Pevzner PA. 2016. hybridSPAdes: an algorithm for hybrid
772 assembly of short and long reads. Bioinformatics 32:1009–1015.

773 80. Seemann T. 2014. Prokka: rapid prokaryotic genome annotation. Bioinformatics 30:2068–2069.

774 81. Arkin AP, Cottingham RW, Henry CS, Harris NL, Stevens RL, Maslov S, Dehal P, Ware D, Perez
775 F, Canon S, Sneddon MW, Henderson ML, Riehl WJ, Murphy-Olson D, Chan SY, Kamimura RT,
776 Kumari S, Drake MM, Brettin TS, Glass EM, Chivian D, Gunter D, Weston DJ, Allen BH, Baumohl
777 J, Best AA, Bowen B, Brenner SE, Bun CC, Chandonia J-M, Chia J-M, Colasanti R, Conrad N,
778 Davis JJ, Davison BH, DeJongh M, Devoid S, Dietrich E, Dubchak I, Edirisinghe JN, Fang G,
779 Faria JP, Frybarger PM, Gerlach W, Gerstein M, Greiner A, Gurtowski J, Haun HL, He F, Jain R,
780 Joachimiak MP, Keegan KP, Kondo S, Kumar V, Land ML, Meyer F, Mills M, Novichkov PS, Oh T,
781 Olsen GJ, Olson R, Parrello B, Pasternak S, Pearson E, Poon SS, Price GA, Ramakrishnan S,

Ranjan P, Ronald PC, Schatz MC, Seaver SMD, Shukla M, Sutormin RA, Syed MH, Thomason J, Tintle NL, Wang D, Xia F, Yoo H, Yoo S, Yu D. 2018. KBase: The United States Department of Energy Systems Biology Knowledgebase. Nat Biotechnol 36:566–569.

82. Bolger AM, Lohse M, Usadel B. 2014. Trimmomatic: a flexible trimmer for Illumina sequence data. Bioinformatics 30:2114–2120.

83. Lai H-Y, Zhang Z-Y, Su Z-D, Su W, Ding H, Chen W, Lin H. 2019. iProEP: A computational predictor for predicting promoter. Molecular Therapy - Nucleic Acids 17:337–346.

84. Kanehisa M, Sato Y, Morishima K. 2016. BlastKOALA and GhostKOALA: KEGG tools for functional characterization of genome and metagenome sequences. J Mol Biol 428:726–731.

Supporting Material

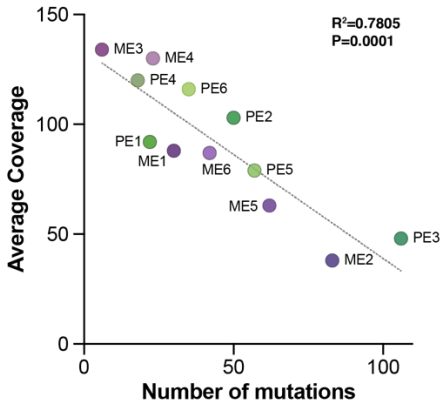

Figure S1. Comparison of the average genome coverage and the number of mutations detected. Dashed lines represent a simple linear regression, and the correlation strength and significance were tested using the Pearson correlation coefficient.

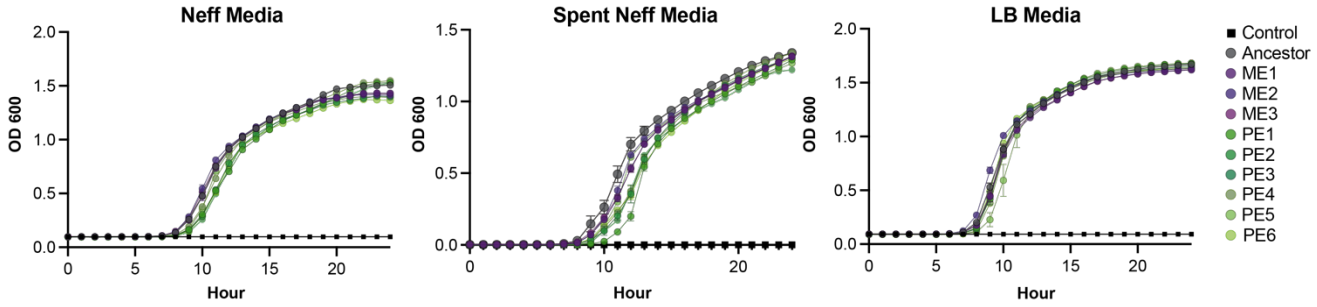

Figure S2. Mean growth rate of each variant based on 600nm OD readings every hour for 24h of ME (purple circles) and PE (green circles) isolates in LB broth (left) or fresh Neff media (right) compared to the ancestral strain (black circles). Significance was tested using Friedman One-Way ANOVA Repeated Measure Analysis with Dunnett's multiple comparisons test.

804

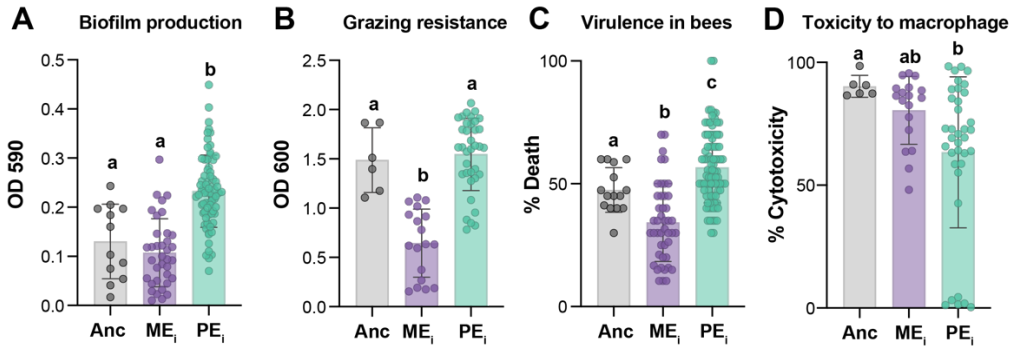

805
806
807 **Figure S3.** Mean A) biofilm production, B) grazing resistance, C) virulence in bees, and D) cytotoxicity to macrophage based
808 on combining all ME and PE isolates. Significance was tested by comparing each evolved isolate to the others and the
809 ancestor using one-way ANOVA with Dunnett's multiple comparisons test.
810

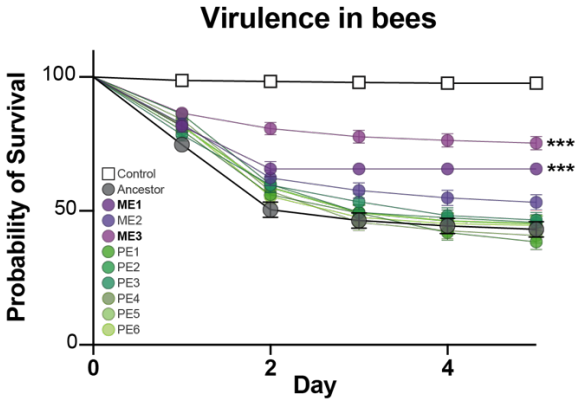

811
812 **Figure S4**. Kaplan-Meier curve showing the probability of survival of honey bees exposed to the ancestral strain (black and
813 gray) and the **A)** ME isolates (purple) and **B)** PE isolates (green). Control bees were given sterile sugar water only (white
814 squares). Mortality was recorded each day for 5 days. Graphs are based on three replicate assays per isolate (n=300 bees per
815 isolate). * = P<0.05, *** = P<0.0005; Mantel-Cox Log-rank test with Bonferroni correction.
816

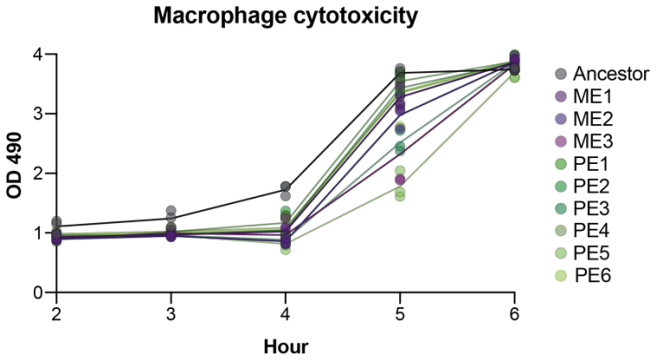

817
818 **Figure S5.** Cytotoxicity of MEi and PEi isolates and the ancestral strain to murine macrophage at an MOI of 1:10
819 (bacteria:macrophage) based on LDH release measured at OD490 after 2h, 3h, 4h, 5h, and 6h co-culture. The assay was
820 done in triplicate. At 6h, death of all macrophage cells (lysis) was observed via microscopy by all evolved isolates as well as
821 the ancestor.

822

823 **Table S1.** Total reads, number of mapped reads, and average genome coverage for each population and isolate.

824

825 **Table S2.** List of all the mutations identified in the evolved isolates and their frequency in the populations.

826

827 **Dataset S1.** List of all the mutations identified in the evolved populations and their frequencies.